



## Comparative Study of The Seismic Performance Between Simply Supported PSC Box Girder Bridge Equipped with Shear Panel Damper and Lead Rubber Bearing

Alvin Kurniawan Santoso<sup>1</sup>, Djoko Sulisty<sup>1</sup>, Ali Awaludin<sup>1\*</sup>, Angga Fajar Setiawan<sup>1</sup>, Iman Satyarno<sup>1</sup>, Sidiq Purnomo<sup>2</sup>, Ignatius Harry<sup>2</sup>

<sup>1</sup>Department of Civil and Environmental Engineering, Universitas Gadjah Mada, Yogyakarta, 55281, Indonesia

<sup>2</sup>Engineering Section, PT. Wijaya Karya Beton Tbk., Boyolali, 57300, Indonesia

**Abstract.** Several bridges in Indonesia are designed using elastomeric bearing (ERB) with a low capability of reducing seismic responses. This results in a significant demand for larger pier cross-sectional dimensions and a greater number of reinforcements, necessitating the consideration of seismic isolation devices to optimize the pier configuration. Lead rubber bearing (LRB) has been widely used as a seismic isolation device due to the natural period shifting and sufficient energy dissipation, but it costs a lot. A shear panel damper equipped with a gap (SPDG) was proposed regarding its capability to provide high damping at low cost as an alternative device to LRB. This study compared the seismic performance of three structural systems of simply supported prestressed concrete (PSC) box girder bridges. Those were analyzed using Nonlinear Time History Analysis (NLTHA) with the OpenSees software. As a result, both SPDG and LRB increased the structural flexibility and generated similar relative pier responses to the conventional bridge with ERB. For example, SPDG generated the relative responses of the top pier displacement, base shear, and bending moment up to 64.76%, 83.55%, and 65.66%, while LRB was 64.92%, 83.39%, and 66.89%, respectively. Meanwhile, the bridge's structural performance equipped with LRB and SPDG showed a fully operational and operational limit, while the one with ERB reached the life safety limit due to the longitudinal earthquake. The life safety limit due to the transverse earthquake was also observed in the three bridge models. In conclusion, SPDG is applicable in the seismic isolation system as it has a similar performance to the LRB.

**Keywords:** Elastomeric Rubber Bearing; Lead Rubber Bearing; Nonlinear Time History Analysis; Simply supported bridge; Shear Panel Damper Plus Gap

### 1. Introduction

The role of seismic isolation devices is crucial in accommodating the deformation of superstructures caused by earthquake forces. Unfortunately, many bridges in Indonesia are equipped with elastomeric bearings (ERB), which have low damping and limited seismic capacity. This leads to a significant force demand being transmitted to the piers (Xiang, Goto, and Alam, 2021; Xiang, Alam, and Li, 2019) and increases the cross-sectional area as well as the number of pier reinforcements to provide uniform seismic resistance. To optimize the

\*Corresponding author's email: [ali.awaludin@ugm.ac.id](mailto:ali.awaludin@ugm.ac.id), Tel.: +62-264-545676; Fax: +62-274-589659  
doi: [10.14716/ijtech.v15i5.5750](https://doi.org/10.14716/ijtech.v15i5.5750)

design and minimize pier damage, it is necessary to utilize seismic isolation devices with high damping, such as lead rubber bearings (LRB) (Edalathi and Tahghighi, 2019; Sugihardjo *et al.*, 2010). Meanwhile, despite the fact that Indonesia is an earthquake-prone area, many practicing engineers would rather use ERB instead of LRB due to budget constraint. This increases the anxiety of many people regarding the structural safety during strong earthquakes. Besides, the application of LRB would require more effort for design and manufacture. Therefore, this study proposed a shear panel damper equipped with a gap (SPDG), as it has a low cost with high damping and a large seismic capacity (Nakashima *et al.*, 1994) to overcome the disadvantages of LRB. Moreover, the proposed device could be easily replaced without lifting the superstructure because the installation was accompanied by other devices that provided vertical load capacity (Xiang, Alam, and Li, 2019).

LRB acts as a bilinear elastic-plastic (Hameed *et al.* 2008; Naeim and Kelly, 1999) with maximum deformation of 250% (Hamaguchi *et al.*, 2019; AASHTO, 2014). Meanwhile, the behavior of the shear panel damper (SPD) is influenced by its web, which is typically constructed using low-yield or mild steels with high ductility, allowing it to deform easily up to a certain deformation limit (Yao, Wang, and Zhu 2021; Zhang *et al.*, 2013). In a study conducted by Liu, Aoki, and Shimoda (2013), it was found that SPD with a square plate and flange deformed by 16-25%. Awaludin *et al.* (2022) developed SPD with a rectangular hollow shape that laterally deformed up to 15% of the body height, and a stable post-yield resistance was obtained when the web depth-thickness ratio was 25. Furthermore, the SPD's web was vulnerable to buckle due to the vertical load and needed to be supported by ERB to provide an equitable vertical load capacity. This ERB also provides lateral stiffness with 100% maximum deformation in the elastic behavior (Yenidogan, 2021). Setiawan and Takahashi (2018) also found that the use of gaps in friction dampers reduced the structural stiffness without any force resistance below the gap length. This simply means that the gap needs to be applied to SPD to increase structural flexibility (Setiawan, 2018).

The previous study concluded that the application of LRB increased the flexibility of a simply supported bridge and protected the pier from more severe damage (Santoso *et al.*, 2022; Santoso, 2022). In this study, three structural systems of simply supported prestressed concrete (PSC) box girder bridges are compared using numerical analysis. This bridge is located in Makassar, Indonesia, and is classified as a critical bridge according to SNI 2833:2016 (BSN, 2016). Several analytical methods have been employed to investigate seismic performance, such as Nonlinear Time History Analysis (NLTHA), pushover analysis, and modal analysis. NLTHA was performed to simulate the structure's dynamic response by applying five selected and scaled ground motion records. A pushover analysis was conducted to determine the actual pier's capacity, while a modal analysis was performed to obtain structural flexibility.

## 2. Methods

### 2.1. Bridge Modeling

The bridge has a total length of 340 m and is supported by a series of single piers of different heights, as shown in Figure 1. A total of three bridge systems were considered in this analysis, which include a conventional bridge equipped with ERB (Model A), an existing bridge equipped with LRB (Model B), and the proposed bridge equipped with the combination of SPDG and ERB (Model C), as shown in Figure 2. The Model B was redesigned with the conventional system of Model A and the proposed system of Model C to provide an equitable seismic resistance with comparable seismic performance. The number of bearings in Model A was determined based on the demand earthquake force, which was

calculated manually using elastic design assumptions for the critical bridge according to SNI 2833:2016 and AASHTO (2012). The design concept for seismic devices in Models B and C followed the guidelines of AASHTO (2014) and was also based on a previous study conducted by Chen, Ge, and Usami (2007). The basis is that the yield strength of the bearing systems should be less than the pier so that the yielding initially occurs at the bearings. Furthermore, the demand force should be less than the maximum force capacity of the bearing system to avoid sliding failure (Chen and Duan, 2014; Steelman *et al.*, 2013) due to the low seismic capacity of ERB, thereby necessitating  $9 \text{ m}^2$  of cross-sectional area and 136 D32 steel bars. Meanwhile, Models B and C required  $6.25 \text{ m}^2$  of cross-sectional area and 110 D32 steel bars.

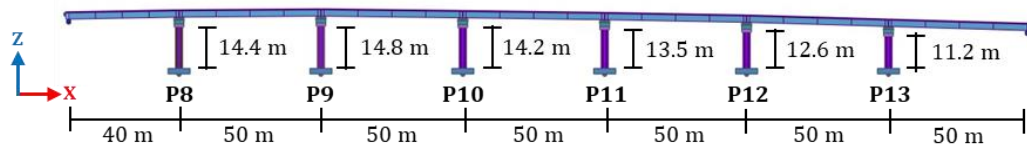


**Figure 1** Longitudinal section of bridge model

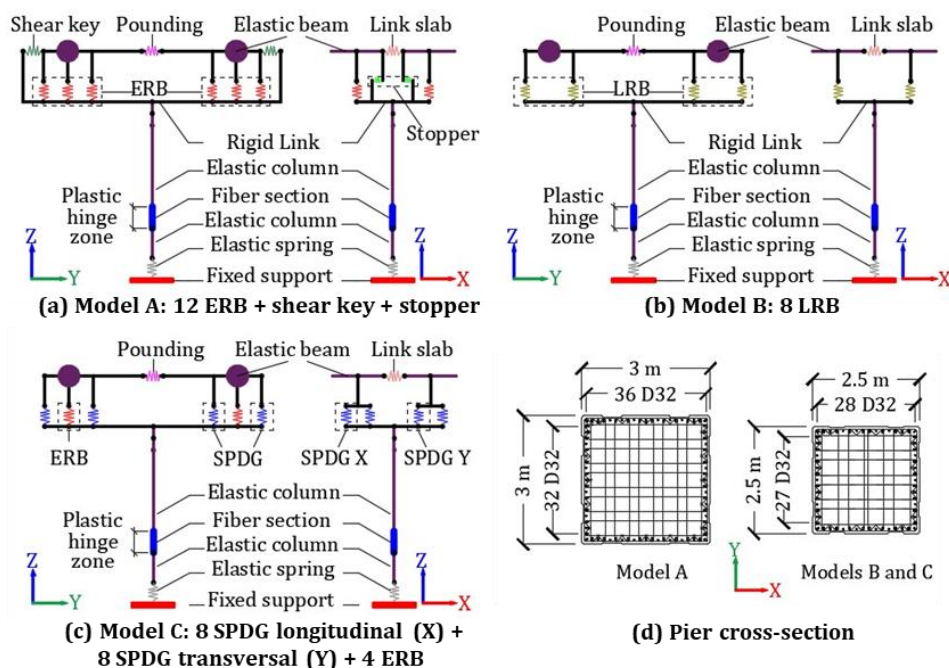


**Figure 2** Bridge model: (a) Model A, (b) Model B, (c) Model C, and (d) Pier cross-section

According to the previous study (Santoso *et al.*, 2022), the structural elements were idealized as force-based beam-column elements with elastic cross-sections. The plastic hinge zone was particularly discretized as fiber to represent the nonlinear pier's behavior (Kappos *et al.*, 2012; Berry and Eberhard, 2008). The concrete materials were idealized using Concrete04, while those in compression and tension behavior were actualized based on Mander Priestley, and Park(1988) and Vecchio and Collins (1986), respectively. The reinforcing steel parameters are defined according to Giuffre-Menegotto-Pinto's model (Fillipou *et al.*, 1983; Menegotto and Pinto, 1973) as Steel02 (Carreno *et al.*, 2019), which has unlimited maximum strain. The stopper, shear key, and pounding effect at the gap of 200 mm were idealized using EPPGap to maintain elastic behavior after the pounding occurrence (Omrani *et al.*, 2015). The link slab was modeled with Concrete01 along the debonded zone without considering tensile behavior, while the foundation was represented by elastic spring elements. The force-displacement relationship of ERB was idealized using an elastic-linear material, while that of LRB was idealized using Steel01.

Meanwhile, SPDG was idealized by combining Steel01 for SPD and EPPGap with the gap length of 15 mm using series material in OpenSees. A scheme of the SPDG mechanism based on [Setiawan and Takahashi \(2018\)](#) is presented in Figure 3.

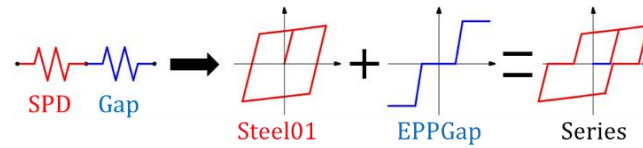


**Figure 3** SPDG mechanism based on [Setiawan and Takahashi \(2018\)](#)

### 2.2. Ground Motion Modification

Five selected earthquakes were classified as far-fault events, as the bridge is situated in Makassar with an epicentral distance exceeding 10 km from the earthquake source. This classification is based on the deaggregation analysis of the Makassar earthquake as outlined in the study conducted by [Sunardi and Nugraha \(2016\)](#). [ASCE \(2010\)](#) allows for the selection of the ground motion by considering the respective similar spectral shape of the designed bridge in such a way that the allowable range of magnitude ( $M_w$ ), fault distance ( $R$ ), source mechanism, and site class were relaxed. Moreover, the magnitude, which is  $\geq 5$ , fault distance  $\leq 500$  km, and shallow crustal mechanism (strike-slip and reverse) were still considered based on the BMKG earthquake repository described by [Sunardi and Nugraha \(2016\)](#) as a lack of references on the deaggregation of Makassar earthquake. Meanwhile, site class D of soil represented by  $V_{s30}$  in the range of 175–350 m/s was determined based on the soil investigation report of the specific bridge location. The amplitude scaling method was used to modify the ground motion selected, and a single scale factor was applied to preserve the variation of earthquake energy with the fundamental period found in the original record ([ASCE, 2017](#); [ASCE, 2010](#); [Kalkan and Chopra, 2010](#)).

### 2.3. Limit State

The performance level is an indicator for observing and evaluating the structural performance simultaneously and an instrument for ensuring structural capability during service life. [NCHRP \(2013\)](#) classified the performance level into five categories, also known as damage levels, as shown in Table 1. The determination of the level depends on several parameters, which include steel strain, concrete strain, and drift ratio. The damage levels I to IV are still repairable. Meanwhile, level V required component replacement. So, the performance level of fully operational (FO), operational (O), life safety (LS), near collapse (NC), and collapse limits (C) are equivalent to damage levels.

**Table 1** Seismic performance and damage level according to [NCHRP \(2013\)](#)

Damage Level	Performance Level	Steel Strain	Concrete Strain	Drift Ratio (%)
I	Fully operational	0.0038	0.0024	0.75%
II	Operational	0.005	0.0032	1.00%
III	Life safety	0.019	0.010	3.00%
IV	Near collapse	0.048	0.027	5.00%
V	Collapse	0.063	0.036	8.70%

## 3. Results and Discussion

### 3.1. Structural Systems Comparison

This study incorporated three parameters as design criteria for predicting the seismic responses of isolated structures. These parameters are the stiffness ratio, yield strength ratio, and ultimate strength ratio, which are utilized to control the seismic behavior. Furthermore, pushover analysis was used to determine the pier strength and stiffness

parameters, while the formula proposed by AASHTO (2014) and Chen, Ge, and Usami (2007) were used to calculate the seismic device.

The pier's elastic stiffness was observed to be less than the effective stiffness of all seismic devices because its ratio exceeded one, as shown in Figure 4(a). However, the energy dissipation started when the yield and the inelastic deformation occurred in the seismic device. In Figure 4(b), the yield strength ratios of Models B and C were below one, meaning that the initial yield of the structural system occurred in the seismic devices rather than the pier. The ratio between the maximum strength of the seismic devices and the pier is shown in Figure 4(c), of which the ratios of Models B and C were above one. This implies the pier potentially collapsed before the seismic devices failed. This makes the design of an optimal isolated bridge system based on the basic concept to be difficult, as the demand force has to be calculated to prevent the devices from failing. Meanwhile, the yield strength ratio was considered an appropriate design approach for seismic isolation devices.

The application of seismic isolation devices increased the structural flexibility represented by the fundamental period. This implies the fundamental period of Model A, being 2.15 s was the smallest. Meanwhile, Models B and C have fundamental periods of 2.50 s and 2.35 s, respectively, implying that the bridge system with LRB was the most flexible, and the application of SPDG also increased the natural period of the bridge system.

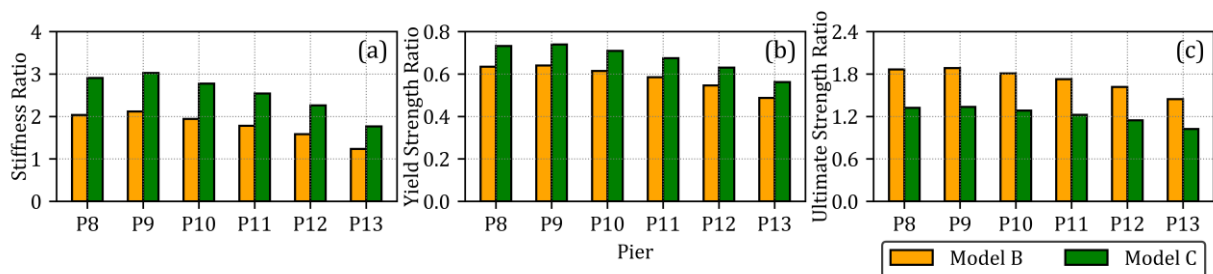


**Figure 4** (a) stiffness ratio, (b) yield strength ratio, (c) ultimate strength ratio

### 3.2. Dynamic Responses Comparison

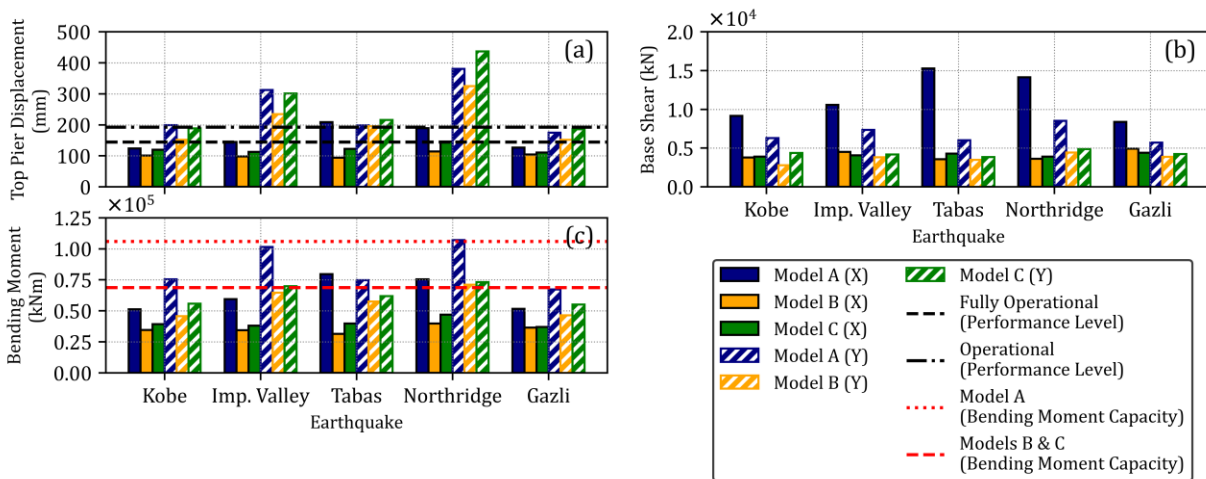
The effectiveness of the seismic isolation device application was evaluated by considering the maximum relative percentage of the pier responses, such as displacement, base shear, and bending moment. The percentage was calculated by comparing the maximum responses of the seismic-equipped bridge systems in Models B and C with the conventional bridge system in Model A. The results of Models A and B were obtained from Santoso *et al.* (2022), while Model C was compared to the previous results.

Figure 5(a) shows a comparison of the maximum top pier displacement in three models, represented by pier P9. It was observed that the longitudinal displacements were smaller compared to the transverse. In this case, all piers have rectangular cross-sections with the same stiffness in both lateral directions, as shown in Figure 2(d). Therefore, the reason is that a free cantilever pier in the transverse direction provided less stiffness than those in the longitudinal that was supported by a series of piers. Furthermore, the longitudinal displacements in Model A were the largest of the other models, but some transverse displacements in Model C were larger than in Model A based on some earthquakes. This was influenced by the larger lateral stiffness and the yield strength ratio of the bearing system to the substructure, where Model C was larger than Model B, as shown in Figure 4. Besides, the bridge system with SPDG generated the maximum relative displacement of 64.76% and 36.75%, while the one with LRB showed 64.92% and 45.92% in the longitudinal and transverse directions, as shown in Table 2.

Models B and C consistently show lower base shear results compared to Model A, as shown in Figure 5(b). The seismic devices were capable of reducing the spectral

acceleration, while the larger pier in Model A produced stiffer piers, thereby resulting in a greater base shear than the other models. Meanwhile, both Models B and C showed comparable relative base shear, as summarized in Table 3. The relative base shears in Models B and C reached 83.39% and 83.55% in the longitudinal directions, as well as 63.66% and 60.60% in the transverse directions, respectively. In manual calculation, the maximum shear capacity of Model A pier was 38740.32 kN, while Models B and C piers were 27377.12 kN. It was observed that the piers in all models did not exceed the maximum shear capacity, meaning that the shear yielding did not occur.

Based on Figure 5(c), Model A showed the largest bending moment in both directions. The flexural capacity of Model A, i.e. 105986.75 kNm, as well as Models B and C, which was 68858.42 kNm, was exceeded in pier P9 due to the Northridge earthquake. This means that flexural yielding was also found in the three models, but the use of LRB in Model B generated relative bending moments up to 66.89% and 48.58% in the longitudinal and transverse directions, as presented in Table 4. Similarly, in Model C, in which the relative bending moments were up to 65.56% and 45.40% in the longitudinal and transverse directions, respectively.



**Figure 5** Maximum (a) top pier displacement, (b) base shear, and (c) bending moment comparison in pier P9

**Table 2** Top pier relative displacement in longitudinal (X) and transverse (Y) directions

Model	Maximum Relative Displacement X (%)						Maximum Relative Displacement Y (%)					
	P8	P9	P10	P11	P12	P13	P8	P9	P10	P11	P12	P13
B	58.2	55.2	57.7	56.7	55.6	64.9	28.9	24.8	45.9	24.7	44.1	28.0
C	55.2	41.3	40.7	34.7	35.6	64.8	13.5	5.4	36.8	7.2	28.0	17.7

**Table 3** Relative base shear in longitudinal (X) and transverse (Y) directions

Model	Maximum Relative Base Shear X (%)						Maximum Relative Base Shear Y (%)					
	P8	P9	P10	P11	P12	P13	P8	P9	P10	P11	P12	P13
B	76.4	76.7	77.1	78.7	81.3	83.4	60.5	55.9	56.5	58.5	63.7	61.4
C	74.7	72.5	72.7	74.8	78.5	83.6	54.0	43.3	50.7	50.3	60.6	58.9

**Table 4** Relative bending moment in longitudinal (X) and transverse (Y) directions

Model	Maximum Relative Bending Moment X (%)						Maximum Relative Bending Moment Y (%)					
	P8	P9	P10	P11	P12	P13	P8	P9	P10	P11	P12	P13
B	60.6	60.5	61.5	60.7	59.8	66.9	43.2	39.4	48.6	40.1	44.2	39.1
C	58.2	50.1	50.1	45.5	46.2	65.6	32.4	31.7	45.4	29.7	39.6	32.6

### 3.3. Seismic Performance and Damage Comparison

The top pier displacement and curvature responses are two indicators for measuring pier performance and damage. Table 5 shows the summary of the maximum top pier displacements and performance levels in each pier. It was observed that Models B and C showed better performances compared to Model A, particularly in the longitudinal direction. This means that fully operational limits were obtained in Models B and C, while Model A was in the life safety limit state. It is important to note that life safety limit states were also observed in all models due to the transverse earthquakes. In addition, damage levels I and II were displayed in Models B and C, while damage level III was shown in Model A due to longitudinal earthquakes. Table 5 also shows that all bridge models reached damage level III due to transverse earthquakes. Therefore, the application of SPDG was able to provide comparable performance and protect the pier from more severe damage, just as in the bridge equipped with LRB.

**Table 5** Maximum performance level in Pier P8 – P13

Model	Maximum Top Pier Displacement (mm)						Maximum Curvature, $\phi \times 10^{-3}$ (rad/m)					
	P8	P9	P10	P11	P12	P13	P8	P9	P10	P11	P12	P13
A-X	204	209	204	182	182	175	1.08	1.09	1.13	1.05	1.11	1.18
B-X	123	114	110	106	99	76	0.86	0.68	0.69	0.68	0.65	0.42
C-X	134	146	143	138	133	122	0.96	1.05	1.08	1.10	1.15	1.19
A-Y	229	381	386	295	305	154	1.33	5.16	6.17	3.34	4.49	1.01
B-Y	179	325	262	248	176	118	1.36	4.96	3.30	3.34	1.61	1.03
C-Y	200	437	345	325	220	144	1.65	9.04	6.31	6.30	2.99	1.42
Performance/Damage Level		FO / I		O / II		LS / III		NC / IV		C / V		

### 3.4. Seismic Device Responses

Hysteretic behavior was exhibited by LRB and SPDG, indicating that yielding and energy dissipation occurred in all seismic devices. The ERB in Model C accommodated the seismic force before the displacement reached a gap length of 15 mm. Furthermore, the SPD and ERB parallel systems worked together to accommodate the earthquake force until a certain deformation limit was reached. The maximum deformation of SPD was set at about 15% as the lower bound based on several deformation limits obtained from experimental studies. However, the gap in SPDG increased the maximum shear strain from 15% to 18%. It also caused the pinched hysteretic curve of SPDG due to zero lateral strength and stiffness along the gap length, as illustrated in Figure 3. Figure 7 shows the responses of seismic devices, which are represented at Pier P9 due to the transverse earthquakes. It was observed that both SPDG and LRB performed well under multiple cycles during all earthquakes without exceeding the deformation limit, indicating that the devices dissipated seismic energy. In this case, LRB still performs better and is more effective at dissipating energy. The maximum force and displacement of LRB provided a larger hysteretic area than SPDG, indicating greater seismic energy dissipated by LRB than SPDG.

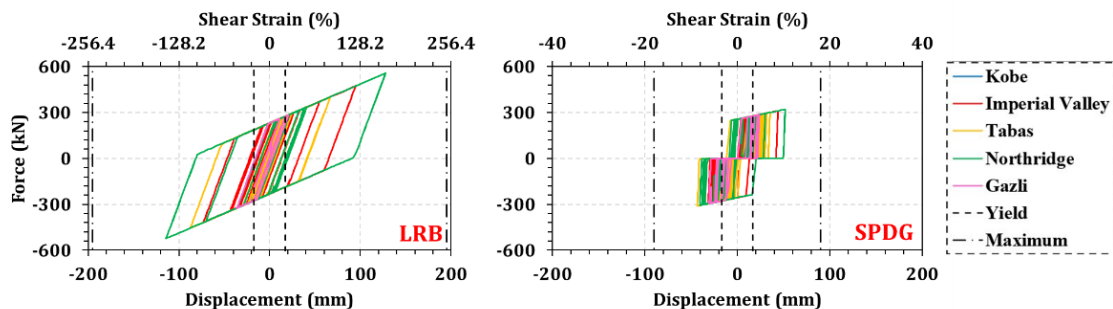


**Figure 7** Seismic device's responses on pier P9 due to the transverse earthquakes

#### 4. Conclusions

Three bridge models with different structural systems have been investigated in this study using numerical analysis. The results showed that the bridge models with seismic devices, such as SPDG and LRB, were more flexible compared to the conventional bridge equipped with ERB. Basically, SPDG started to dissipate seismic energy when the deformation exceeded the gap length then the metal web experienced yielding. The yielding state initiated an inelastic behavior that provided low post-yield stiffness to accommodate the superstructure's deformation. Meanwhile, the designed gap allowed the device to deform at a zero-stiffness state that increased the maximum shear strain capacity by 3% to prevent failure. As a result, piers in the bridge with SPDG have comparable responses to LRB. The relative responses to the conventional bridge, i.e., top pier displacement, base shear, and bending moment, generated up to 64.76%, 83.55%, and 65.66%, while LRB generated up to 64.92%, 83.39%, and 66.89%, respectively. The practical design of isolated bridges with SPDG was also made easy when the appropriate parameters were defined based on the target performance. Therefore, the yield strength ratio needs to be considered as a criterion for designing the SPDG and predicting the structural responses due to seismic excitation. It was observed that the bridge with SPDG, which was designed in the yield strength ratio's range of 0.53–0.73, showed comparable seismic performance to the bridge with LRB. Those were fully operational and operational limits due to the longitudinal earthquakes, and life safety limit due to the transverse earthquakes. In addition, the influence of vertical direction earthquakes will increase vertical deformation. Consequently, the friction between two-separated plates on the top of SPDG potentially occurred. This might inflict a large buckling displacement and influenced the hysteretic behavior. Thus, it should be considered while designing the vertical gap of SPDG.

#### Acknowledgments

The authors are grateful to the Department of Civil and Environmental Engineering at Universitas Gadjah Mada and PT. Wijaya Karya Beton Tbk. for the data support.

#### References

- American Association of State Highway and Transportation Officials (AASHTO), 2012. *LRFD Bridge Design Specifications*. American Association of State Highway and Transportation Officials, Washington, USA
- American Association of State Highway and Transportation Officials (AASHTO), 2014. *Guide Specifications for LRFD Seismic Bridge Design*, 2<sup>nd</sup> Edition. American Association of State Highway and Transportation Officials. Washington, USA
- American Society of Civil Engineers (ASCE), 2010. *ASCE 7-10: Minimum Design Loads for Buildings and Other Structures*. American Society of Civil Engineers, Virginia, USA
- American Society of Civil Engineers (ASCE), 2017. *ASCE 7-16: Seismic Evaluation and Retrofit of Existing Buildings*. American Society of Civil Engineers, Virginia, USA
- Awaludin, A., Setiawan, A.F., Satyarno, I., Wu, S., Haroki, Y., 2022. Finite Element Analysis of Bi-directional Shear Panel Damper with Square Hollow Section under Monotonic Loading. *Journal of the Civil Engineering Forum*, Volume 8(2), pp. 157–168
- Badan Standardisasi Nasional (BSN), 2016. *SNI 2833:2016 Seismic Design of Bridge*. Badan Standardisasi Nasional, Jakarta, Indonesia
- Berry, M.P., Eberhard, M.O., 2008. Performance Modeling Strategies for Modern Reinforced Concrete Bridge Columns. Report PEER 2007/07, Pacific Earthquake Engineering Research Center, Berkeley, California

- Carreno, R., Lotfizadeh, K.H., Conte, J.P., Restrepo, J.I., 2019. Material Model Parameters for The Giuffre-Menegotto-Pinto Uniaxial Steel Stress-Strain Model. *Journal of Structural Engineering*, Volume 146, pp. 1 – 21
- Chen, W., Duan, L., 2014. *Bridge Engineering Handbook 2<sup>nd</sup> Edition, Seismic Design*. CRC Press, New York, USA
- Chen, Z., Ge, H., Usami, T., 2007. Study on Seismic Performance Upgrading for Steel Bridge Structures by Introducing Energy-dissipation Members. *Journal of Structural Engineering*, Volume 53A, pp. 540–549
- Edalathi, A.A., Tahghighi, H., 2019. Investigating The Performance of Isolation Systems in Improving the Seismic Behavior of Urban Bridge. *Archives of Civil Engineering*, Volume 65, pp. 155 – 175
- Fillippou, F., Popov, E., Bertero, V., 1983. *Effects of Bond Deterioration on Hysteretic Behavior of Reinforced Concrete Joints*. Report EERC 83-19, Pacific Earthquake Engineering Research Center, Berkeley, California
- Hamaguchi, H., Wake, T., Yamamoto, M., Kikuchi, M., 2019. Practical Application of Lead Rubber Bearings with Fail-safe Mechanism. *Journal of Structural and Construction Engineering*, Volume 12, pp. 187 – 196
- Hameed, Koo, M., Do, T.D., Jeong, J. Effect of Lead Rubber Bearing Characteristics on The Response of Seismic-isolated Bridges. *KSCE Journal of Civil Engineering*, Volume 12(3), pp. 187-196
- Kalkan, E., Chopra, A.K., 2010. Practical Guidelines to Select and Scale Earthquake Records for Nonlinear Response History Analysis of Structures. Report 2010-1068, U.S. Geological Survey, California, USA
- Kappos A.J., Saiidi, M.S., Aydinoglu, M.N., Isacovic, T., 2012. *Seismic Design and Assessment of Bridges*, Springer, New York, USA
- Liu, Y., Aoki, T., Shimoda, M., 2013. Strain Distribution Measurement of a Shear Panel Damper Developed for Bridge Structure. *Journal of Structures*, Volume 2013, pp. 1–11
- Mander, J.B., Priestley, M.N.J., Park, R., 1988. Theoretical Stress-strain Model for Confined Concrete. *Journal of Structural Engineering*, Volume 144, pp. 1804-1826
- Menegotto, M., Pinto, P., 1973. Method of Analysis for Cyclically Loaded RC Plane Frames Including Changes in Geometry and Non-elastic Behavior of Elements Under Combined Normal Force and Bending. IABSE Symposium on Resistance and Ultimate Deformability of Structure Acted on by Well Defined Repeated Loads: Proceeding, Volume 11, pp. 15 – 22
- Naeim, F., Kelly, J.M., 1999. *Design of Seismic Isolated Structures: From Theory to Practice*. John Wiley & Sons Inc., New York, USA
- Nakashima, M., Iwai, S., Iwata, M., Takeuchi, T., Konomi, S., Akazawa, T., Saburi, K., 1994. Energy Dissipation Behavior of Shear Panels Made of Low Yield Steel. *Earthquake Engineering and Structural Dynamics*, Volume 23, pp. 1299-1313
- National Cooperative Highway Research Program (NCHRP), 2013. *Performance-Based Seismic Bridge Design: A Synthesis of Highway Practice*. Transportation Research Board, Washington, USA
- Omran, R., Mobasher, B., Liang, X., Gunay, S., Mosalam, K.M., Zareian, F., Taciroglu, E., 2015. Guidelines for Nonlinear Seismic Analysis of Ordinary Bridge: Version 2.0. Report No. 15-65A0454, California Department of Transportation, California, USA
- Santoso, A., Sulistyono, D., Awaludin, A., Setiawan, A.F., Satyarno, I., Purnomo, S., Harry, I., 2022. Structural Systems Comparison of Simply Supported PSC Box Girder Bridge Equipped with Elastomeric Rubber Bearing and Lead Rubber Bearing. *Civil Engineering Dimension*, Volume 24, pp. 19–30

- Santoso, A.K., 2022. Perbandingan Penggunaan Shear Panel Damper dan Lead Rubber Bearing untuk Meningkatkan Performa Seismik Struktur Jembatan Box Girder Tumpuan Sederhana (*Comparative Study on Seismic Performance Between Simply Supported Box Girder Bridge Equipped with Shear Panel Damper and Lead Rubber Bearing*). Master's Thesis, Graduate Program, Universitas Gadjah Mada, Yogyakarta, Indonesia
- Setiawan, A.F., 2018. Development of High Seismic Performance Integrated Bridge Pier Connected by Hysterical Damper, Doctor's Dissertation, Graduate Program, Kyoto University, Kyoto, Japan
- Setiawan, A.F., Takahashi, Y., 2018. A High Seismic Performance Concept of Integrated Bridge Pier with Triple RC Columns Accompanied by Friction Damper Plus Gap. *Journal of Japan Society of Civil Engineers*, Volume 74, pp. 131-147
- Steelman J., Fahnestock, L., Filipov, E., LaFave, J., Hajjar, J., Foutch, D., 2013. Shear and Friction Response of Nonseismic Laminated Elastomeric Bridge Bearings Subject to Seismic Demands. *Journal of Bridge Engineering*, Volume 18, pp. 612 - 623
- Sugihardjo, H., Tavio, Manalu, I., Lesmana, Y., 2018. Seismic Study of Lead-Rubber Bearing Application in Kutai Kertanegara Steel Arch Bridge. *International Journal on Advanced Science Engineering Information Technology*, Volume 8, pp. 540 - 546
- Sunardi, B., Nugraha, J., 2016. Peak Ground Acceleration at Surface and Spectral Acceleration for Makassar City Based on A Probabilistic Approach. *Jurnal Meteorologi dan Geofisika*, Volume 17, pp 33-46
- Vecchio, F.J., Collins, M.P., 1986. The Modified Compression-field Theory for Reinforced Concrete Elements Subject to Shear. *Journal Proceedings*, Volume 83, pp. 219-231
- Xiang, N., Alam, M., Li, J., 2019. Yielding Steel Dampers as Restraining Devices to Control Seismic Sliding of Laminated Rubber Bearings for Highway Bridges: Analytical and Experimental Study. *Journal of Bridge Engineering*, Volume 24(11), pp. 1-15
- Xiang, N., Goto, Y., Alam, M., Li, J., 2021. Effect of Bonding or Unbonding on Seismic Behavior of Bridge Elastomeric Bearings: Lessons Learned from Past Earthquakes in China and Japan and Inspirations for Future Design. *Advances in Bridge Engineering*, Volume 2(1), pp. 1-17
- Yao, Z., Wang, W., Zhu, Y., 2021. Experimental Evaluation and Numerical Simulation of Low-yield-point Steel Shear Panel Dampers. *Engineering Structures*, Volume 245, pp. 1-17
- Yenidogan, C., 2021. Earthquake-Resilient Design of Seismically Isolated Buildings: A Review of Technology. *Vibration*, Volume 4, pp. 602-647
- Zhang, C., Zhang, Z., Aoki, T., Zhang, M., 2013. Research on The Dynamic Performance of Low-Yield-Strength Shear Panel Damper for Bridge Application. *Journal of Shanghai Jiaotong University*, Volume 18, pp. 118-128